

# Loss of Fibroblast Thy-1 Expression Correlates with Lung Fibrogenesis

James S. Hagood,\*† Priya Prabhakaran,\*  
Pallavi Kumbha,\* Lorena Salazar,\*  
Mark W. MacEwen,\* Thomas H. Barker,‡  
Luis A. Ortiz,§ Trenton Schoeb,¶  
Gene P. Siegal,†||\*\* C. Bruce Alexander,||  
Annie Pardo,†† and Moisés Selman‡‡

From the Departments of Pediatrics,\* Cell Biology,† Genomics and Pathobiology,¶ Pathology,|| and Surgery,\*\* University of Alabama, Birmingham, Alabama; the Department of Environmental and Occupational Health,§ Graduate School of Public Health, University of Pittsburgh, Pittsburgh, Pennsylvania; the Laboratory of Regenerative Medicine and Pharmacobiology,‡ Ecole Polytechnique Fédérale de Lausanne, Lausanne, Switzerland; the Facultad de Ciencias,†† Universidad Nacional Autónoma de México, Mexico City, Mexico; and the Instituto Nacional de Enfermedades Respiratorias,‡‡ Mexico City, Mexico

**Fibroblasts consist of heterogeneous subpopulations that have distinct roles in fibrotic responses. Previously we reported enhanced proliferation in response to fibrogenic growth factors and selective activation of latent transforming growth factor (TGF)- $\beta$  in fibroblasts lacking cell surface expression of Thy-1 glycoprotein, suggesting that Thy-1 modulates the fibrogenic potential of fibroblasts. Here we report that compared to controls Thy-1 $-/-$  C57BL/6 mice displayed more severe histopathological lung fibrosis, greater accumulation of lung collagen, and increased TGF- $\beta$  activation in the lungs 14 days after intratracheal bleomycin. The majority of cells demonstrating TGF- $\beta$  activation and myofibroblast differentiation in bleomycin-induced lesions were Thy-1-negative. Histological sections from patients with idiopathic pulmonary fibrosis demonstrated absent Thy-1 staining within fibroblastic foci. Normal lung fibroblasts, in both mice and humans, were predominantly Thy-1-positive. The fibrogenic cytokines interleukin-1 and tumor necrosis factor- $\alpha$  induced loss of fibroblast Thy-1 surface expression *in vitro*, which was associated with Thy-1 shedding, Smad phosphorylation, and myofibroblast differentiation. These results suggest that fibrogenic injury promotes loss of lung fibroblast Thy-1 expression, resulting in enhanced fibrogenesis. (Am J Pathol 2005, 167:365–379)**

Idiopathic pulmonary fibrosis (IPF), with its histopathological signature of usual interstitial pneumonia (UIP), is a paradigmatic, but as yet primarily enigmatic example of uncontrolled fibroproliferation. IPF is remarkable for its insidious onset, dramatic histopathological and pathophysiological derangements, and relentless progression to death regardless of treatment. The etiology of IPF, and the factors that direct its dismal outcome, remain the subject of intense investigation.<sup>1</sup> Fibroblasts are the cellular *sine qua non* of fibrosis in most tissues, and the histopathology of IPF underscores this observation. The histopathological feature most clearly correlated with outcome is the presence in lung of fibroblastic foci of young connective tissue, the presence of which portends death within months.<sup>2</sup> Fibroblastic foci seem to represent the fibroproliferative leading edge of the heterogeneous areas of scarring in IPF.<sup>3–5</sup> The myofibroblasts within these foci are clearly dysregulated in their proliferative and matrix-productive function, yet the origin of these cells, and the factors that lead to their accumulation and persistence, are unknown.

Fibroblasts in most tissues are heterogeneous with respect to size, secretory profile, and surface markers. Fibroblasts within a fibrogenic milieu clearly differ from those in normal tissues. In particular, fibroblasts isolated from lungs with active fibrotic disease have increased proliferative capacity, are capable of anchorage-independent growth, and are morphologically distinct.<sup>6–8</sup> Furthermore, differences among subsets of normal fibroblasts have been identified on the basis of surface markers, cytoskeletal composition, lipid content, and cytokine profile.<sup>9</sup> One of the most extensively characterized experimental models of fibroblast heterogeneity is based on surface expression of Thy-1 glycoprotein. Thy-1-negative and Thy-1-positive mouse lung fibroblasts differ morphologically and have differing cytokine secretory pro-

Supported in part by the National Institutes of Health (grants HL-03239 and AR-20614-24; grant ES-10859 to L.A.O.; and Research Facilities Improvement Program grant no. C06 RR 15490 from the National Center for Research Resources) and the American Lung Association (Career Investigator Award to J.S.H.).

Accepted for publication April 26, 2005.

Address reprint requests to James S. Hagood, M.D., UAB Pediatric Pulmonology and Cell Biology, 648A VH, 1670 University Blvd., Birmingham, AL 35294-0019. E-mail: jhagood@peds.uab.edu.

files.<sup>9–11</sup> Based on our previous observations of enhanced *in vitro* proliferative responses of Thy-1-negative fibroblasts to fibrogenic mediators,<sup>12,13</sup> and our recent finding that Thy-1 limits the ability of fibroblasts to activate latent transforming growth factor (TGF)- $\beta$  and express  $\alpha$ -smooth muscle actin ( $\alpha$ -SMA),<sup>14</sup> we hypothesized that the absence of Thy-1 correlates with enhanced fibrogenesis.

Thy-1 $^{-/-}$  mice are viable and have normal life expectancy; however neither fibrosis nor wound healing have been previously explored in these animals. In this study we describe a marked increase in severity of lung fibrosis in response to intratracheal bleomycin (BL) in Thy-1 $^{-/-}$  mice. Furthermore, in human lung tissues from individuals with IPF/UIP, the myofibroblasts in fibroblastic foci are Thy-1-negative, despite the fact that the majority of fibroblasts from normal lung are Thy-1-positive. Incubation of human lung fibroblasts with cytokines and growth factors important in the initiation or progression of fibrosis results in decreased Thy-1 surface expression concurrent with increased evidence of TGF- $\beta$  signaling and myofibroblastic differentiation. Taken together, these findings suggest that Thy-1-negative fibroblasts have an increased propensity to fibrogenic responses, consistent with their *in vitro* phenotype, and that a profibrotic milieu may shift fibroblasts toward a Thy-1-negative phenotype. This is thus the first description of a correlation of the absence of fibroblast Thy-1 to fibrosis in murine models and in human patient material.

## Materials and Methods

### Materials

Formalin-fixed, paraffin-embedded lung tissue was obtained from biopsy or autopsy specimens of individuals with clinical pulmonary fibrosis (Instituto Nacional de Enfermedades Respiratorias, Mexico City, Mexico, and University of Alabama–Birmingham Hospital, Birmingham, AL), in compliance with institutional review board-approved protocols, and in accordance with principles set forth in the Declaration of Helsinki. Informed written consent was obtained from all patients. Diagnosis of IPF was supported by history, physical examination, pulmonary function studies, high-resolution computed tomography, and bronchoalveolar lavage, and was corroborated by open lung biopsy. The morphological diagnosis of IPF was based on typical microscopic findings of UIP. IPF patients fulfilled the diagnostic criteria of the American Thoracic Society and the European Respiratory Society. Diagnosis of hypersensitivity pneumonitis was suspected based on recurrent symptoms after exposure to a known offending antigen, positive precipitating antibodies to the offending antigen, and characteristic findings on high-resolution computed tomography and bronchoalveolar lavage,<sup>15,16</sup> and was confirmed by characteristic findings on histology.<sup>17</sup> Human lung- and skin-derived primary fibroblasts (CCL-204, CRL-1491, CRL-2076) were obtained from the American Type Culture Collection (Rockville, MD). Additional normal human lung fibroblasts (LN-1) at low passage were the kind gift of Pro-

fessor David Abraham, University College London, London, UK. Antibodies used were as follows: anti-human Thy-1/CD90 [MCAP90 (Serotec, Inc., Raleigh, NC) or catalog no. 555595 (BD Pharmingen, San Diego, CA), or sc-9163 (Santa Cruz Biotechnology, Santa Cruz, CA)]; anti-human prolyl-4-hydroxylase  $\beta$  (N631641; ICN, Inc., Costa Mesa, CA); anti-human proliferating cell nuclear antigen (PCNA, M0879; DAKO, Inc., Carpinteria, CA); anti-human vimentin (MCA 459F; Serotec, Inc.); anti-human  $\alpha$ -SMA (immunofluorescence, immunohistochemistry: Sigma Chemical, St. Louis, MO; immunoblotting: BioCarta, San Diego, CA); anti-phosphorylated Smad 2/3 (Cell Signaling Technology, Beverly, MA); anti-total Smad 2/3 (BD Transduction Laboratories, San Diego, CA); rabbit polyclonal antibody specific to the active form of TGF- $\beta$  (LC-1-30-1; a kind gift of Dr. Kathy Flanders, National Cancer Institute, Bethesda, MD<sup>18</sup>); rabbit pan-specific antibody to total TGF- $\beta$ 1, -2, -3 (R&D Systems, Inc., Minneapolis, MN); anti- $\beta$ -tubulin (Santa Cruz Biotechnology); and anti-BrdU (BD Pharmingen). Nonimmune rabbit IgG or antibody to trinitrophenol were used as control antibodies for immunohistochemical staining and flow cytometry (03000D and 03004C, BD Pharmingen). Cytokines and growth factors, recombinant mouse interleukin (IL)-1 $\beta$ , and tumor necrosis factor (TNF)- $\alpha$  were obtained from R&D Systems.

### Thy-1 $^{-/-}$ Mice

All animal studies were performed in accordance with Institutional Animal Care and Use Committee-approved protocols. Thy-1 gene-targeted mice were generated on a C57BL/6 background by insertion of a neomycin resistance gene (Neo) into the third exon of the Thy-1 gene.<sup>19</sup> Dr. Michael Bloom at the National Heart, Lung, and Blood Institute (NHLBI, Bethesda, MD) kindly provided Thy-1 $^{-/-}$  breeding pairs for this project, and a colony of these mice is maintained in our animal facility. Representative mice were examined by the UAB Health Surveillance/Diagnostic Laboratory and found to be free of a panel of 19 murine viral and bacterial pathogens and *Mycoplasma pulmonis*.

Thy-1 $^{-/-}$  and age-matched wild-type (WT) mice were anesthetized with ketamine/xylazine intraperitoneally. The trachea was exposed, and BL (Calbiochem, La Jolla, CA) or sterile saline (NS) was injected intratracheally in a volume of 2  $\mu$ l/g body weight (4 U/kg dose BL). The neck wound was closed with wound clips and the animals were returned to microisolator cages and allowed free access to feed and water. A subset of WT mice was injected with BrdU (1 mg, BD Pharmingen) 90 minutes before sacrifice. At 14 days, the thoracic cage was opened under anesthesia and the animals exsanguinated. The left bronchus was ligated, and the left lung removed for hydroxyproline analysis. The right lung was fully inflated with alcoholic formalin at a constant pressure of 15-cm H<sub>2</sub>O for 30 minutes. After fixation, lungs were embedded in paraffin, sectioned at 5  $\mu$ m, and stained on separate glass slides with hematoxylin and eosin (H&E), picrosirius red, and Masson's trichrome, or processed for immunohistochemistry (IHC). In BrdU-injected mice, the

lungs were inflated with optimum cutting temperature (OCT) medium, embedded in OCT, and snap-frozen in isopentane precooled in liquid nitrogen. Cryostat sections (4  $\mu\text{m}$ ) were obtained for immunofluorescence staining.

### Morphometric Analysis

Picrosirius red-stained sections were examined by an investigator (M.W.M.) who was blinded to the experimental conditions, using an Olympus BX-51 microscope with polarizing light filter, and imaged using a Spot charge-coupled device (CCD) camera (Diagnostic Instruments, Inc., Sterling Heights, MI). Morphometric analysis of the birefringent signal from picrosirius red-stained collagen was performed using a modification of previously described methods,<sup>20</sup> using Bioquant Nova software (Bioquant Image Analysis Corp., Nashville, TN). Briefly, whole lung sections are visualized at  $\times 2$  and the lung tissue outlined. Five random regions of interest of  $500 \times 500 \mu\text{m}$  are selected from peribronchial regions, and 10 regions of interest are selected from alveolar regions, by an observer (M.W.M.) blinded to the experimental conditions. Bright pixels in dark-field images, representing collagen, were selected by thresholding and determined as a percentage of total pixels, averaged throughout the regions of interest. For analysis of IHC staining for active and total TGF- $\beta$ , whole lung sections were visualized at  $\times 100$  using a Nikon Labophot microscope by an investigator blinded to the conditions and imaged using a QiCam fast-cooled CCD color camera at high resolution ( $1392 \times 1040$  pixels). Metamorph software version 6.2 r4 (Universal Imaging Corp., Downingtown, PA) was used to define threshold for positive antibody staining in comparison with nonimmune serum controls. Positive pixels were expressed as a percentage of total tissue area, averaged over six random fields per sample.<sup>21,22</sup>

### Hydroxyproline Analysis

Left lungs were dissected free of large airways, weighed, minced, and subjected to acid hydrolysis in 6 N HCl (2 ml) for 16 hours at  $110^\circ\text{C}$ . The hydrolysate was buffered with an equal volume of 6 N NaOH, filtered, and a measured aliquot removed. Hydroxyproline was converted to pyrrole-2-carboxylic acid by oxidizing the samples with 0.2 mol/L chloramine-T. After 25 minutes, 3.6 mol/L of sodium thiosulfate was added to stop the oxidation. After toluene extraction, Ehrlich's reagent (*p*-diethylaminobenzaldehyde) was added and optical density read by spectrophotometry at 557 nm. Standard 4-hydroxyproline (Sigma Chemical Co.) was used to generate a standard curve and values are expressed as total lung hydroxyproline.<sup>23</sup>

### Histology and IHC

Human lung tissue blocks were cut in 5- $\mu\text{m}$  sections, and adjacent sections were analyzed as follows: H&E staining was performed on every fourth section (ie, first, fifth,

ninth, etc., cut from a block), to correlate immunohistochemical staining to histopathology. After antigen unmasking using 10 mmol/L citric acid at  $90^\circ\text{C}$  for 30 minutes, and blocking with 50% normal goat serum, intervening sections were stained with the following antibodies: mouse anti-human CD90 (Thy-1), mouse anti-human prolyl 4-hydroxylase, mouse anti-human vimentin, mouse anti-human PCNA, mouse anti-human  $\alpha$ -SMA, and with appropriate control antibodies. Sections from mice were stained with anti-phospho Smad 2/3, anti-active TGF- $\beta$ , anti-total TGF- $\beta$ , or control antiserum. Staining was developed with biotinylated secondary antibodies (Southern Biotechnology Associates, Birmingham, AL) and streptavidin-peroxidase (Pierce, Rockford, IL) and either the diaminobenzamide-nickel reaction mixture (Pierce) or 3-amino-9-ethylcarbazole chromogen (Vector Laboratories, Burlingame, CA). Endogenous peroxidase activity was quenched with 3%  $\text{H}_2\text{O}_2$ . Images were obtained with a Spot Insight CCD camera and accompanying software.

### Histopathological Scoring

The H&E- and IHC-stained sections were examined by two experienced anatomical pathologists (G.P.S. and C.B.A.), to determine whether they met diagnostic criteria for UIP,<sup>4</sup> and to determine immunohistochemical staining for CD90 (Thy-1). Numbered mouse sections (H&E and Masson's trichrome) were examined by an experienced veterinary pathologist (T.R.S.) who was blinded to the experimental conditions. Lesions were scored according to a modification of previously described methods for inflammatory lesions in murine lungs,<sup>24,25</sup> taking into account both the extent of tissue involvement and the types and severity of changes within affected areas. For inflammation, individual changes scored were septal macrophages, luminal macrophages, septal neutrophils, luminal neutrophils, septal lymphocytes, luminal lymphocytes, epithelial hypertrophy and hyperplasia, epithelial sloughing, septal edema, luminal proteinic material (edema, fibrin deposition), multinucleate giant cells, perivascular mononuclear cells, and focal lymphocyte accumulation in areas of consolidation and fibrosis. Each was assigned a value of 0, 1, 2, or 3 for absent, mild, moderate, or severe, respectively. The sum of these values was multiplied by 1, 2, 3, or 4, for, respectively, <25%, 25% to 50%, 50% to 75%, or >75% or more of the area of the tissue section affected, yielding an inflammation score. A fibrosis score was calculated similarly, using the criteria of fibroblast proliferation, collagen formation, and collapse and obliteration of alveolar spaces. Scoring was based on H&E sections, except collagen formation, which was scored from duplicate sections stained with Masson's trichrome.

### Fibroblast Culture and Cytokine Exposure

Normal human skin or lung fibroblast lines at low passage (<P8) were cultured at  $37^\circ\text{C}$  in Dulbecco's minimum essential medium with 10% fetal bovine serum. Cells were grown in six-well dishes, 100-mm dishes, or on

glass coverslips to ~80% confluency, then rendered quiescent for 48 hours in medium containing 0.1% fetal bovine serum. Mediators ( $n = 3$  for each mediator/time point) were added in serum-free medium (SFM) for 1, 3, 6, 24, 48, 72, and 96 hours. For mediator exposures beyond 24 hours, mediators were added in fresh medium every 24 hours. In a subset of cells, after a 96-hour exposure to cytokines, the monolayers were washed three times with SFM and cultured an additional 72 hours in SFM without added cytokines.

### *Flow Cytometry*

Cells were removed from dishes by trypsinization, resuspended in wash buffer, and analyzed by fluorescence-activated cell sorting as previously described, using either fluorescein isothiocyanate (FITC)-conjugated anti-CD90 or FITC-conjugated isotype control.<sup>12</sup>

### *Annexin V and Propidium Iodide Staining*

Unfixed fibroblasts grown on glass coverslips and treated as described above were processed for detection of cell surface phosphatidylserine expression using FITC-conjugated Annexin V, and for detection of disrupted membrane integrity using propidium iodide, by means of the Annexin V-FITC apoptosis detection kit (Medical and Biological Laboratories Co., Ltd., Woburn, MA), according to the manufacturer's instructions. Fibroblasts were then stained for Thy-1 using mouse anti-human CD90 (Serotec) or isotype control at 1:20, 4°C × 18 hours, then fixed in 3% formaldehyde for 15 minutes and followed by Texas Red X-conjugated F(ab') secondary antibody for 1 hour at room temperature. After mounting, coverslips were observed using a Nikon TE200U inverted fluorescence microscope and imaged using a CoolSnap HQ 12 Bit CCD camera (Photometrics, Tucson, AZ). Cycloheximide (100 μmol/L)-treated fibroblasts were used as positive controls for Annexin V staining.

### *Thy-1 Immunoprecipitation*

Thy-1 was immunoprecipitated from conditioned media from stimulated fibroblasts using anti-human Thy-1 polyclonal antibody or control antiserum conjugated to protein A/G Sepharose beads, after preclearing with non-conjugated beads. Beads were washed four times with 0.1% Triton X-100, 50 mmol/L Tris-Cl, pH 7.4, 300 mmol/L NaCl, 5 mmol/L ethylenediamine tetraacetic acid, 0.02% sodium azide at 4°C, once with phosphate-buffered saline (PBS) at 4°C, resuspended in nonreducing sodium dodecyl sulfate-polyacrylamide gel electrophoresis (SDS-PAGE) sample buffer, boiled 5 minutes, and subjected to SDS-PAGE. Proteins were transferred to polyvinylidene difluoride membranes and subjected to standard immunoblotting for Thy-1. Blots were developed using enhanced chemiluminescence and digital images were obtained using a BioChem Digital CCD camera (UVP Bioimaging Systems, Upland, CA) and analyzed using LabWorks software (UVP Bioimaging Systems). In-

tensity of Thy-1-specific bands, which were not present in control immunoprecipitation lanes, was quantified and averaged for triplicate samples.

### *Immunoblotting*

Fibroblasts grown in 100-mm dishes were treated with cytokines as described above. Protein from whole cell lysates prepared in the presence of protease inhibitors was loaded onto 10% SDS-PAGE gels at 25 μg per lane, based on Bradford assay (Pierce Chemical Co., Rockford, IL), and separated electrophoretically along with markers of known molecular weight. Protein was transferred onto polyvinylidene difluoride filters that were blocked with 3% milk/PBS and probed with antibody to α-SMA (1:1000). Horseradish peroxidase-conjugated secondary antibodies for all immunoblots were used at 1:10,000. The filters were then developed with an enhanced chemiluminescent detection system and autoradiographs generated. Autoradiographs were imaged and analyzed using the Kodak 1D image analysis system (Eastman-Kodak, Rochester, NY). Filters were stripped and reprobed with antibody to β-tubulin (1:400). For determination of total and phosphorylated Smad 2/3, cell lysates prepared in the presence of 1.0 mmol/L Na orthovanadate (Sigma), before SDS-PAGE (40 μg cell lysate protein/well) and immunoblotting with phosphorylation-specific antibodies to Smad 2/3 (1:1000), then stripped and reprobed with antibody to total Smad (1:2000).

### *Reverse Transcriptase-Polymerase Chain Reaction (RT-PCR)*

Total RNA was prepared from stimulated fibroblast monolayers using RNeasy (Qiagen, Inc., Valencia, CA), and integrity of RNA determined by agarose gel electrophoresis and ethidium bromide staining. One μg of total RNA was reverse-transcribed and subjected to PCR amplification using the SuperScript III One-Step RT-PCR system (Invitrogen, Inc., Carlsbad, CA) with the following primers: human Thy-1 forward: 5'-TCGTAGCGAGAGGAC-GATTG-3', human Thy-1 reverse: 5'-GGAGGAGG-GAGAGGGACAGC-3', yielding a 445-bp fragment; and human glyceraldehyde-3-phosphate dehydrogenase (GAPDH; constitutive internal control) forward: 5'-CCAC-CCATGGCAAATTCCATGGCA-2' identical to positions 212 to 235, and reverse: 5'-TCTAGACGGCAGGTCAG-GTCCACC-3', complimentary to positions 786 to 809, yielding a 600-bp fragment. Thy-1 and GAPDH were amplified together using the following cycling parameters: 15 minutes at 95°C, then cycled 28 times at 94°C for 30 seconds, 55°C for 60 seconds, and elongated at 72°C for 60 seconds. Optimal number of cycles to yield linear increase in PCR products was previously determined. After amplification the PCR products were separated on a 2% agarose gel containing 0.3 μg/ml of ethidium bromide and bands visualized and analyzed using Kodak 1D imaging system and software (Kodak) and the ratio of the

density of Thy-1 to GAPDH was then calculated for triplicate samples.

### Immunofluorescence

Cryostat sections from mouse lungs were rinsed in PBS and incubated overnight at 4°C in FITC-conjugated rat anti-mouse CD90.2 or isotype control at 1:20, then fixed in 3% formaldehyde, permeabilized in 0.5% Triton-X100, blocked in 10% normal goat serum, and incubated with either anti- $\alpha$ -SMA (1:400), anti-phosphorylated Smad 2/3 (1:500), anti-active TGF- $\beta$  (1: 400), or control antiserum (1:500), followed by Texas Red X-conjugated secondary antibody (1:200). Nuclei were counterstained with Hoechst 33258, and slides were washed and mounted using ProLong anti-fade reagent (Molecular Probes, Eugene, OR). Fluorescence microscopy and imaging was as described above for Annexin V staining. For color photomicrographs, monochrome images for green, red, and blue fluorescence were obtained individually using appropriate bandpass filters and merged using MetaMorph software (Universal Imaging Corp.). For BrdU immunofluorescence, cryostat sections were processed using the BrdU *In Situ* detection kit (BD Pharmingen) according to the manufacturer's instructions. Human fibroblasts grown on coverslips were fixed and permeabilized as described above for cryostat sections and incubated in FITC-conjugated anti-CD90 (1:20) overnight at 4°C followed by Cy3-conjugated anti- $\alpha$ -SMA (1:400) for 1 hour at room temperature, then counterstained and mounted as described above.

### Statistical Analysis

For interval data generated by morphometric analysis of active TGF- $\beta$  IHC, picrosirius red-stained collagen and hydroxyproline analysis, as well as scoring for inflammation and fibrosis, one-way analysis of variance was used to determine significant differences between groups, with the Holm-Sidak method used for multiple pairwise comparisons. SigmaStat 3.0 software (SPSS, Inc., Chicago, IL) was used for all statistical analyses. Significance was accepted at a level of  $P < 0.05$ . BL-treated animals showing no histopathological change were excluded from analysis. For comparison of Thy-1 expression using flow cytometry data, mean FITC fluorescence for the positive population (M2 in Figure 7D) was averaged for each mediator/time point. One-way analysis of variance and Student's *t*-test were also used to compare data from immunoprecipitation and immunoblotting studies. Significance was accepted at a level of  $P \leq 0.05$ .

## Results

### Thy-1<sup>-/-</sup> Mice Demonstrate Enhanced Fibrosis after Intratracheal BL Compared to WT C57BL/6 Mice

To determine whether fibroblast Thy-1 expression affects fibrotic responses to lung injury, Thy-1<sup>-/-</sup> and

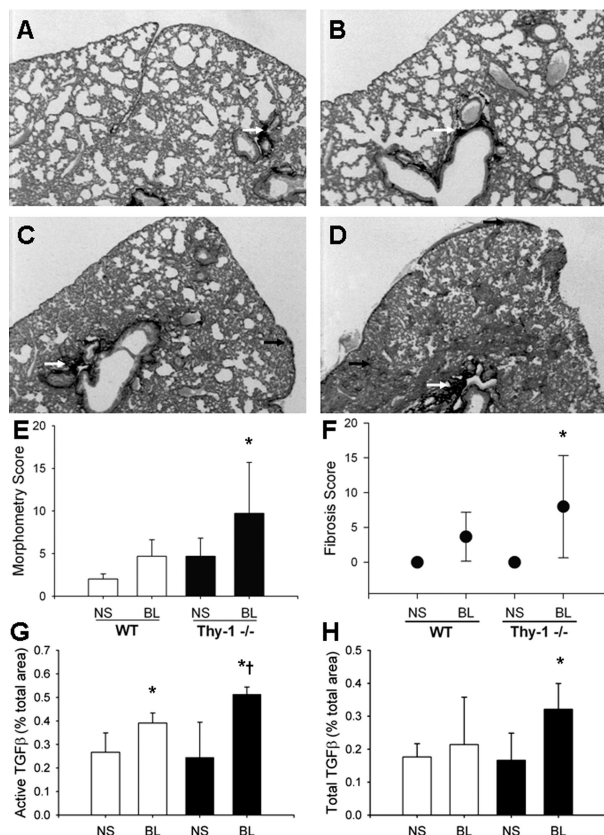


**Figure 1.** Thy-1<sup>-/-</sup> mice have increased fibrosis and lung collagen accumulation after intratracheal BL. **A–D:** Representative picrosirius red-stained 5- $\mu$ m sections of formalin-fixed, paraffin-embedded right lungs of 6-week-old C57BL/6 WT (**A, C**) or Thy-1<sup>-/-</sup> (**B, D**) mice that received intratracheal BL (4 U/kg; **C** and **D**) or an equal volume of normal saline (**A, B**) 14 days previously, as described in Materials and Methods. **White arrows** indicate picrosirius red-stained collagen in peribronchial areas, **black arrows** indicate collagen in subpleural and interstitial areas. **E–H:** Picrosirius red-stained lungs were analyzed under polarized light for morphometric analysis of collagen in a blinded manner as described in Materials and Methods. Mean  $\pm$  SD are shown (**E:** \* $P < 0.01$  for Thy-1<sup>-/-</sup> BL ( $n = 8$ ) versus WT NS ( $n = 5$ ) and Thy-1<sup>-/-</sup> NS ( $n = 8$ ),  $P < 0.05$  versus WT BL ( $n = 8$ )). Trichrome-stained lungs from the same experiment were examined by an experienced veterinary pathologist (T.R.S.) in a blinded manner and assigned a histopathological score for fibrosis as described in Materials and Methods (**F:** \* $P < 0.05$  versus NS-treated controls). IHC staining for active and total TGF- $\beta$  was performed and analyzed using morphometric analysis as described in Materials and Methods (**G:** \* $P < 0.01$  versus NS-treated controls, † $P = 0.012$  versus WT BL; **H:** \* $P < 0.005$  versus all other conditions). Original magnifications,  $\times 2$ .

age-matched control mice of the same strain were given BL intratracheally. Histological analysis of lungs from Thy-1<sup>-/-</sup> mice 14 days after intratracheal BL demonstrated increased fibrosis especially in peribronchial and subpleural locations, as indicated by histopathological changes and staining with picrosirius red and Masson's trichrome, indicating collagen deposition (Figure 1; A to D). BL-treated mice had coalescent multifocal to diffuse alveolitis with accumulation of neutrophils, macrophages, and lymphocytes in alveolar septa and lumina; hypertrophy, hyperplasia, and sloughing of type II alveolar epithelial cells; and multinucleate giant cells in alveolar lumina in severely affected areas. Using a scoring system for inflammation and fibrosis, Thy-1<sup>-/-</sup> mice demonstrated statistically significant fibrosis at 14 days compared to con-

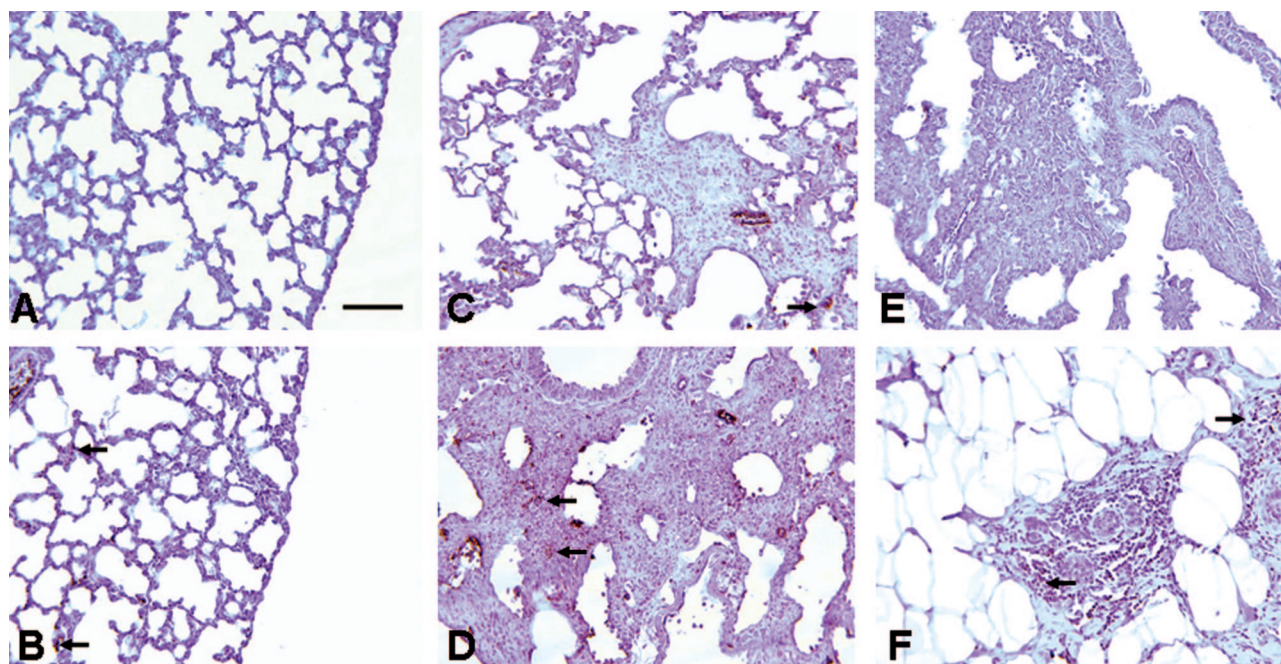


**Figure 2.** Lungs from *Thy-1*<sup>-/-</sup> mice demonstrate increased immunoreactivity for phosphorylated Smad 2/3, indicative of TGF- $\beta$  activity, after intratracheal BL. Photomicrographs of representative (5  $\mu$ m) sections from formalin-fixed, paraffin-embedded right lungs of 6-week-old C57BL/6 WT (A, C) or *Thy-1*<sup>-/-</sup> (B, D) mice that received intratracheal BL (C, D; 4 U/kg) or an equal volume of saline (A, B) 14 days previously, stained with antibody to phosphorylated Smad 2/3 (pSmad2/3), as described in Materials and Methods. **Arrows** indicate areas of strong positivity (dark brown staining). **E:** Section from BL-treated KO mouse from the same experiment, stained with control antiserum; **F:** section from invasive breast carcinoma stained with pSmad2/3 antibody. Scale bar, 100  $\mu$ m. Original magnifications,  $\times 20$ .

trols (Figure 1F,  $P < 0.05$ ). There were no significant differences in inflammation between WT and *Thy-1*<sup>-/-</sup> mice (data not shown). Morphometric analysis of picrosirius red-stained collagen demonstrated more extensive collagen deposition in *Thy-1*<sup>-/-</sup> mouse lungs in peribronchial regions compared to controls ( $P = 0.013$  versus WT BL,  $P = 0.009$  versus WT NS and 0.010 versus *Thy-1*<sup>-/-</sup> NS; Figure 1E). Differences in alveolar septal collagen did not reach statistical significance (not shown). Analysis of lung hydroxyproline content confirmed more extensive collagen deposition in *Thy-1*<sup>-/-</sup> mouse lungs at 14 days compared to controls (*Thy-1*<sup>-/-</sup> BL:  $102.7 \pm 1.5$   $\mu$ g/lung; WT BL:  $62.7 \pm 16.1$ ; *Thy-1*<sup>-/-</sup> NS:  $46.4 \pm 1.7$ ; WT NS:  $55.4 \pm 7$ ;  $P = 0.001$  versus WT BL,  $P < 0.001$  versus WT NS and KO NS). TGF- $\beta$  is the growth factor most strongly associated with fibrotic responses in the lung and many other organs.<sup>26,27</sup> Because we had previously demonstrated activation of latent TGF- $\beta$  only in *Thy-1*-negative fibroblasts,<sup>14</sup> we used an antibody specific to the active form of TGF- $\beta$  for immunohistochemical (IHC) staining in a subset of mice, and analyzed the intensity of staining morphometrically. Figure 1, G and H, shows that there is significantly higher TGF- $\beta$  activity in *Thy-1*-null mice after BL ( $P = 0.012$  versus WT BL). Total TGF- $\beta$  immunostaining (including latent and active forms of isoforms 1, 2, and 3) was also increased significantly in *Thy-1*-null mice after BL ( $P = 0.013$  versus WT BL).

#### *Phosphorylation of Smad 2/3, Indicative of Active TGF- $\beta$ Signaling, Is Increased in *Thy-1*<sup>-/-</sup> Mice after Intratracheal BL*

We determined signaling indicative of TGF- $\beta$  activity in lungs of *Thy-1*<sup>-/-</sup> and WT mice using an antibody for phosphorylated Smad 2/3, which is a specific signaling intermediate downstream of active TGF- $\beta$ .<sup>28</sup> Immunohistochemical staining for pSmad 2/3 demonstrated diffuse, prominent staining in connective tissue cells in fibrotic areas in lungs of *Thy-1*<sup>-/-</sup> mice 14 days after intratracheal BL (Figure 2D), compared with patchy staining in WT mice after BL (Figure 2C). Some interstitial staining was also seen in *Thy-1*<sup>-/-</sup> saline-treated control mice (Figure 2B). Control antiserum did not stain mouse lung sections, and staining of tissue from invasive breast carcinoma (positive control) was strongly positive in the neoplastic cells (Figure 2, E and F).

#### *TGF- $\beta$ Activation, Incorporation of BrdU, and $\alpha$ -SMA Expression Occur in *Thy-1*-Negative Cells in Fibrotic Areas in WT Mice after BL*

We performed immunofluorescent staining for active TGF- $\beta$  in lungs of WT mice 2 weeks after intratracheal BL or normal saline (Figure 3, A and B). Rare cells in fibrotic areas expressed *Thy-1*, and there was no co-localization of *Thy-1* with active TGF- $\beta$ . We also performed immunofluorescent staining of phosphorylated Smad 2/3 (not shown). As for

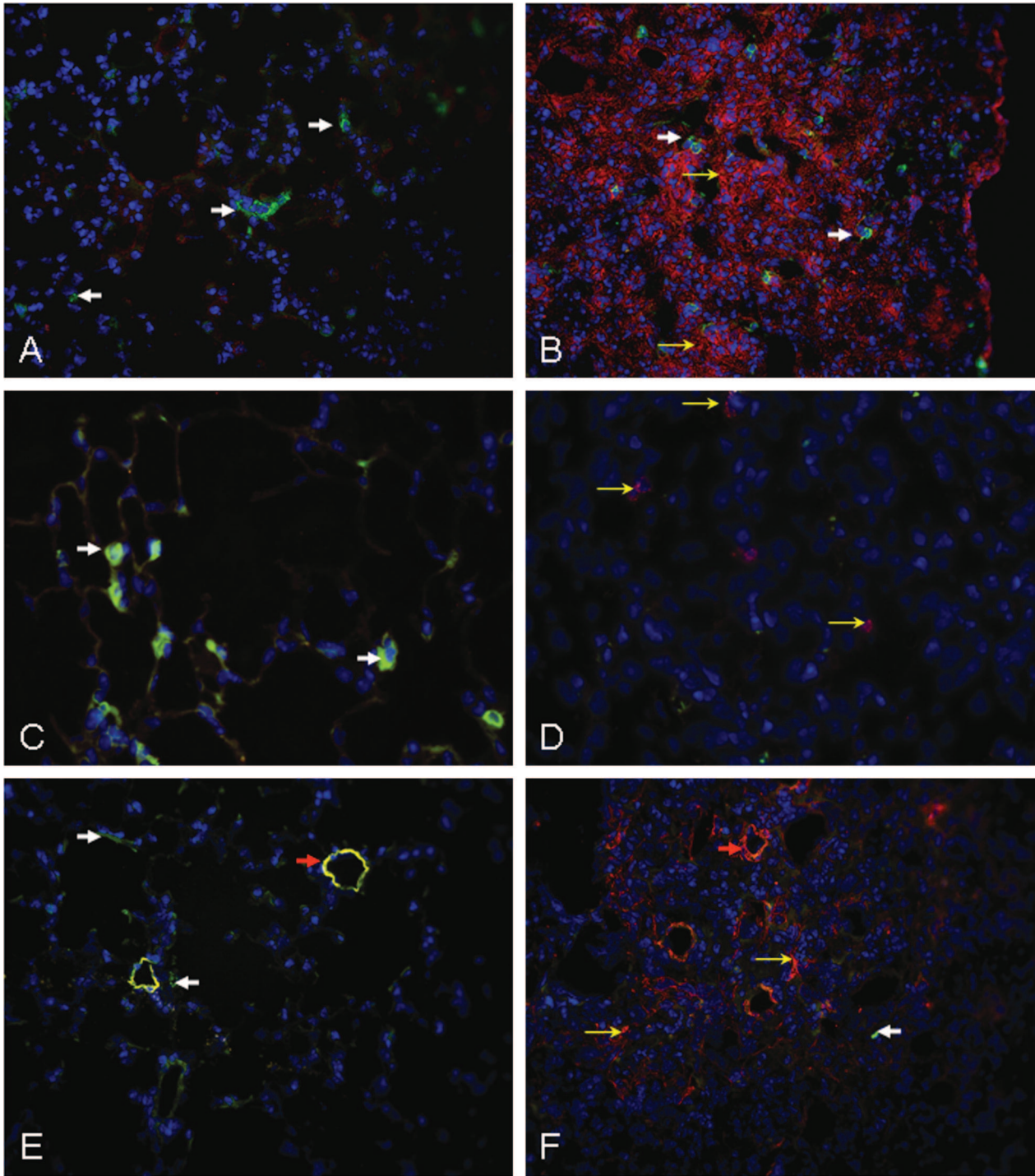


**Figure 3.** Lungs from WT mice demonstrate immunoreactivity for active TGF- $\beta$ , BrdU, and  $\alpha$ -SMA, in cells lacking Thy-1 expression, in fibrotic areas after intratracheal BL. Immunofluorescence photomicrographs of representative ( $4\ \mu\text{m}$ ) cryostat sections from frozen, OCT-embedded lungs of 6-week-old C57BL/6 WT mice that received intratracheal BL (**B, D, F**; 4 U/kg) or an equal volume of saline (**A, C, E**), 14 days previously, and that received 1 mg of BrdU intraperitoneally 90 minutes before sacrifice. All sections were stained with FITC-coupled antibody to Thy-1 (CD90.2, green) and Hoechst 33258 (blue). **A, B:** Sections also stained with active TGF- $\beta$  antibody. **Solid white arrows** indicate Thy-1-positive cells (green), **open yellow arrows** indicate cells positive for active TGF- $\beta$  (red). **C, D:** Sections also stained with BrdU antibody. **Solid white arrows** indicate Thy-1-positive cells (green), **open yellow arrows** indicate BrdU-positive cells (magenta). **E, F:** Sections also stained with  $\alpha$ -SMA antibody. **Solid white arrows** in **E** and **F** indicate Thy-1-positive cells (**E**, green), **open yellow arrows** indicate  $\alpha$ -SMA-positive fibroblasts (**F**, red). **Orange arrows** (**E, F**) indicate small blood vessels in which Thy-1 and  $\alpha$ -SMA co-localize in saline-treated animals (**E**), but only  $\alpha$ -SMA is seen in BL-treated animals (**F**). Original magnifications:  $\times 25$  (**A, B, E, F**);  $\times 40$  (**C, D**).

active TGF- $\beta$ , staining for pSmad 2/3 was absent from control lungs, but diffusely increased in hypercellular fibrotic areas after BL, and did not co-localize with Thy-1. Mice

injected with BrdU 1 hour before sacrifice demonstrated no BrdU staining in the lung after saline, but scattered BrdU-positive cells in fibrotic areas after 14 days of BL (Figure 3,

C and D). Again, there was no co-localization with Thy-1. Saline-treated lungs demonstrated  $\alpha$ -SMA mostly restricted to small arteries, co-localizing with Thy-1. After BL,  $\alpha$ -SMA was diffusely increased in hypercellular fibrotic areas where Thy-1 was mostly absent. No co-localization of Thy-1 with  $\alpha$ -SMA was detected in fibrotic areas.

### *Proliferating Myofibroblasts within Fibroblastic Foci in IPF Are Thy-1-Negative*

Lung tissue from 16 individuals with fibrotic lung disease (12 UIP, 2 hypersensitivity pneumonitis, 2 undetermined with end-stage fibrosis) were examined by two anatomical pathologists blinded to the clinical diagnoses to determine patterns of expression of Thy-1 in fibrotic areas. All sections examined demonstrated absent Thy-1 staining in areas of fibroblastic foci. Trace staining was seen in three UIP specimens and one specimen consistent with hypersensitivity pneumonitis, but in all of these cases immunoreactivity was restricted to inflammatory cells or small blood vessels (Figure 4, B and D). Within fibroblastic foci characteristic of UIP, Thy-1 staining was absent (Figure 4, B and D; Figure 5, A and C). Adjacent sections were stained for prolyl-4 hydroxylase (P4H)  $\beta$ , an essential enzyme for collagen biosynthesis and therefore a sensitive, although not specific, marker for fibroblasts.<sup>29,30</sup> The majority of the spindle-shaped cells within fibroblastic foci were P4H-positive (Figure 4E). Many of these cells were also positive for PCNA (Figure 4F), indicating that these were actively proliferating lesions, consistent with previously published studies.<sup>31</sup> Antibody to vimentin stained multiple nonepithelial cell types in both involved and uninvolved areas of lung, and isotype control antibody staining was appropriately nonreactive (not shown). A subset of samples was stained for  $\alpha$ -SMA. Positive staining was observed in airway and vascular smooth muscle (Figure 5, B and F), and in fibroblastic foci (Figure 5, B and D). Adjacent sections demonstrated absent Thy-1 staining in the same foci (Figure 5, A and C). In areas of dense fibrosis, Thy-1 staining was variable. Figure 5, E and F, demonstrates Thy-1 staining in scattered spindle-shaped cells in areas of dense fibrosis where  $\alpha$ -SMA staining is primarily absent.

### *Normal Lung Fibroblasts Are Predominantly Thy-1-Positive*

Normal lung fibroblasts isolated from uninvolved lung removed during tumor resection, or normal lung fibroblasts obtained from commercial sources, were examined for Thy-1 expression by flow cytometry at low passage number ( $P < 5$ ). The majority of normal lung fibroblasts ( $91.7 \pm 8\%$ ,  $n = 6$ ) expressed Thy-1 in normal culture conditions. In all normal lung sections examined, or in uninvolved areas of IPF lung sections, Thy-1 immunostaining was seen in the alveolar septae (Figure 6, A and B) in locations that were also positive for P4H (Figure 6, C and D), and negative for PCNA (not shown).

### *Human Lung Fibroblasts Exposed to Inflammatory/Fibrogenic Mediators Lose Surface Thy-1 Expression*

Based on the above findings, there appeared to be a change in fibroblast Thy-1 expression associated with fibroblastic foci of IPF/UIP. Therefore, we explored whether cytokines and growth factors known to be important in the pathogenesis of fibrosis, or in the transition from lung injury to fibroproliferation, induced changes in fibroblast Thy-1 expression. Normal fibroblasts were cultured in the presence of interleukin-1 $\beta$  (IL-1), TNF- $\alpha$  (TNF), TGF- $\beta$  (TGF), or fibroblast growth factor-1 (FGF) for specified time intervals up to 96 hours, then examined by flow cytometry. IL-1 and TNF, individually and together caused significant decreases in Thy-1 expression as determined by surface staining with anti-Thy-1 (Figure 7, A and D), as did TGF and FGF (Figure 7A). The decrease was not present at early time points (1, 3, and 6 hours; not shown), but began to be evident at 24 hours and was most evident at 72 hours. A number of different normal lung and skin fibroblasts were tested and showed decreases in Thy-1 expression between 15% and 30% at 72 hours (Table 1). Flow cytometry histograms indicated both a shift in the intensity of Thy-1 staining in Thy-1-positive fibroblasts (Figure 7D; dashed arrow, open arrowhead), and an appearance of Thy-1-negative cells (Figure 7D; dotted arrow, closed arrowhead). Fluorescent staining of identically treated fibroblasts grown on glass coverslips with either Annexin V-FITC or propidium iodide failed to demonstrate significant apoptosis or necrosis after cytokine treatment for 72 hours (not shown). Additional cultures were exposed to IL-1 and TNF, individually or in combination, for 96 hours, then washed with SFM and cultured for an additional 72 hours in SFM. The intensity of Thy-1 staining in cells after 72 hours of cytokine withdrawal did not differ significantly from that of fibroblasts maintained in SFM for an equivalent time interval (Figure 7B), suggesting that at this time interval of exposure, loss of Thy-1 is reversible.

### *Inflammatory Cytokines Induce Accumulation of Soluble Thy-1 in Conditioned Media of Lung Fibroblasts, but No Significant Change in Thy-1 mRNA*

To determine mechanisms for the cytokine-induced decreases in Thy-1 expression, we measured accumulation of Thy-1 in conditioned media. Thy-1 was immunoprecipitated from conditioned media of LN-1 fibroblasts exposed to IL-1, TNF, or both cytokines in combination. At 12 hours, there was an approximately twofold increase in soluble Thy-1 in TNF- and IL-1/TNF-exposed cultures (Figure 7C). IL-1 alone also appeared to cause accumulation of soluble Thy-1, although the quantification did not reach statistical

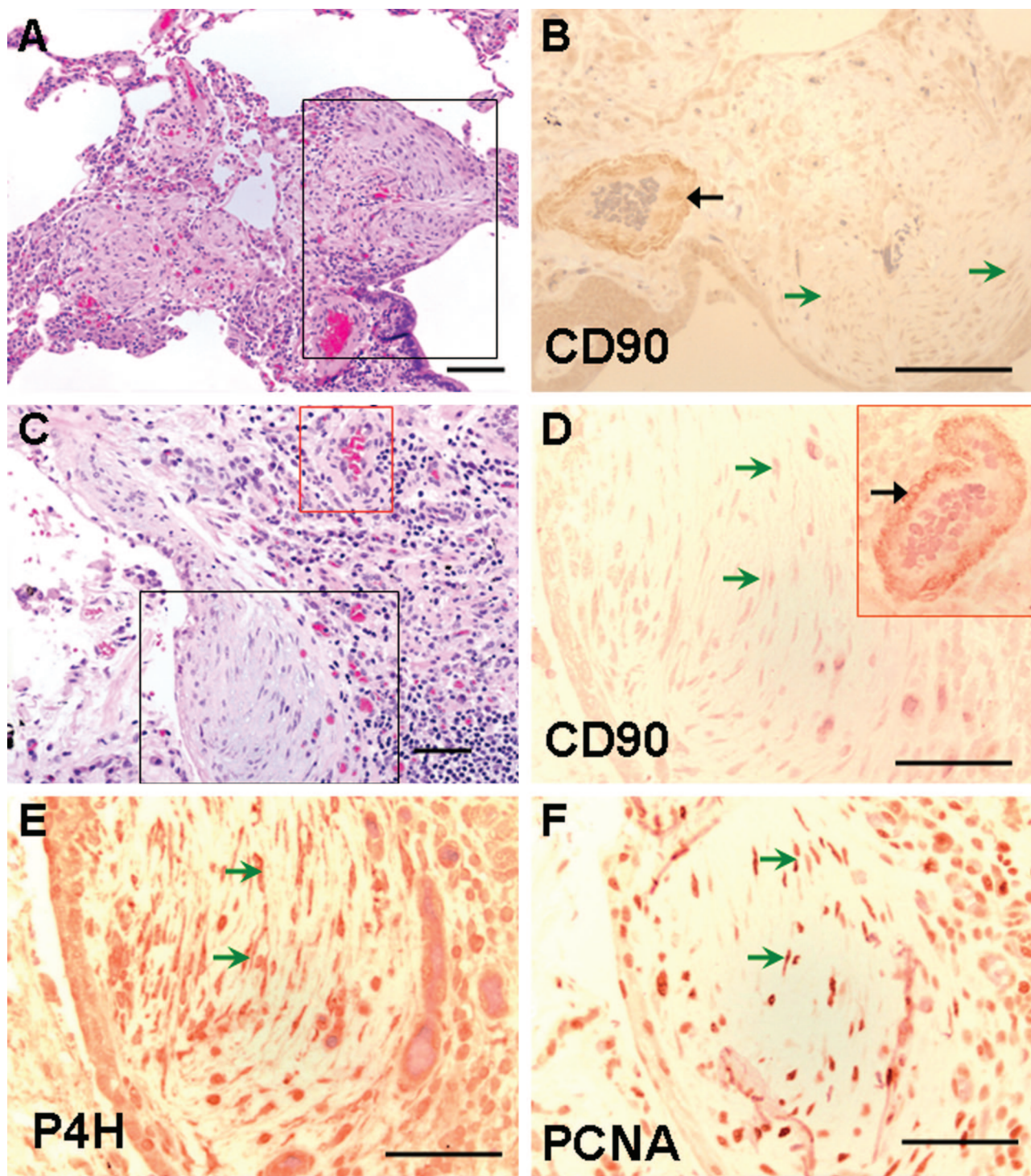


**Figure 4.** Fibroblasts within fibroblastic foci demonstrate absent Thy-1 (CD90) staining. Photomicrographs of serial sections from lung biopsy of two patients with IPF/UIP. **A:** H&E. **Black box** demarcates a fibroblastic focus and correlates to area shown in **B**. **B:** Thy-1 (CD90). Positive immunostaining is seen predominantly in the wall of a vascular structure (**black arrow**). Spindle-shaped cells in fibroblastic foci (**open green arrowheads**) demonstrate absent staining for Thy-1 and are equivalent to isotype control (not shown). **C:** H&E. Section from another IPF patient. **Black box** demarcates a fibroblastic focus and correlates to area shown in **D-F**. **Red box** correlates to **inset** in **D**. **D:** Thy-1 (CD90). Positive immunostaining is seen predominantly in capillaries and in the wall of a vascular structure (artery, **red box**) within the same section (**solid black arrow**). **E:** IHC for P4H. Dark reddish brown staining in spindle-shaped cells indicates fibroblasts (**open green arrowheads**). **F:** IHC for PCNA. Dark reddish brown nuclei indicate proliferating cells (**open green arrowheads**). Scale bars, 132.8  $\mu$ m. Original magnifications:  $\times 10$  (**A**, **C**);  $\times 20$  (**B**, **D-F**).

significance. Total RNA from cytokine-stimulated cultures was subjected to RT-PCR for Thy-1. At 6 hours (Figure 7E) and 12 hours (not shown) there was no

significant change in Thy-1 mRNA levels normalized to the housekeeping gene glyceraldehyde-3-phosphate dehydrogenase (GAPDH).

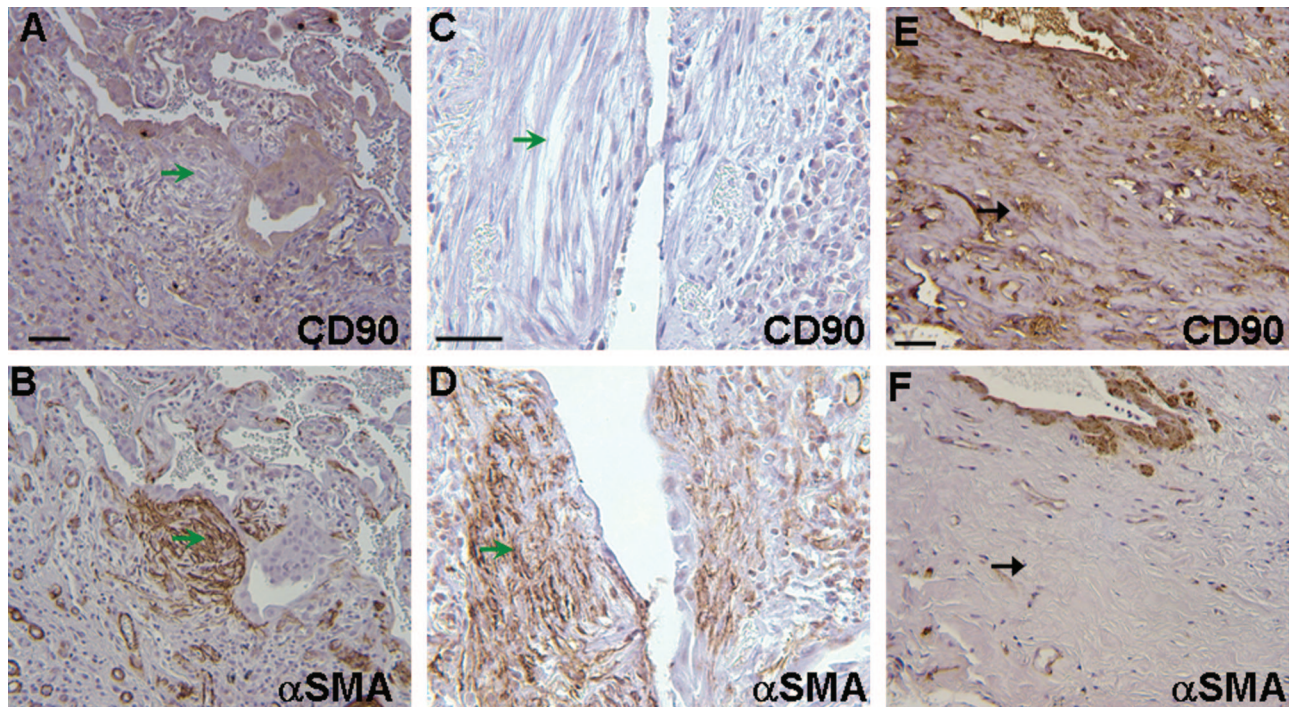


**Figure 5.** Myofibroblasts within fibroblastic foci demonstrate absent Thy-1 staining. Photomicrographs of sections from lung biopsies of three patients with UIP/IPF. **Top:** IHC for Thy-1 (CD90). **Bottom:** IHC for  $\alpha$ -SMA from nearby sections from the same patients. **A–D:** Fibroblastic foci showing absent Thy-1/CD90 staining in myofibroblastic cells (**open green arrowheads**). **E, F:** Area of dense fibrosis showing Thy-1/CD90-positive spindle-shaped cells that are negative for  $\alpha$ -SMA (**solid black arrows**). Scale bar, 50  $\mu$ m. Original magnifications,  $\times 25$  (A, B, E, F);  $\times 40$  (C, D).

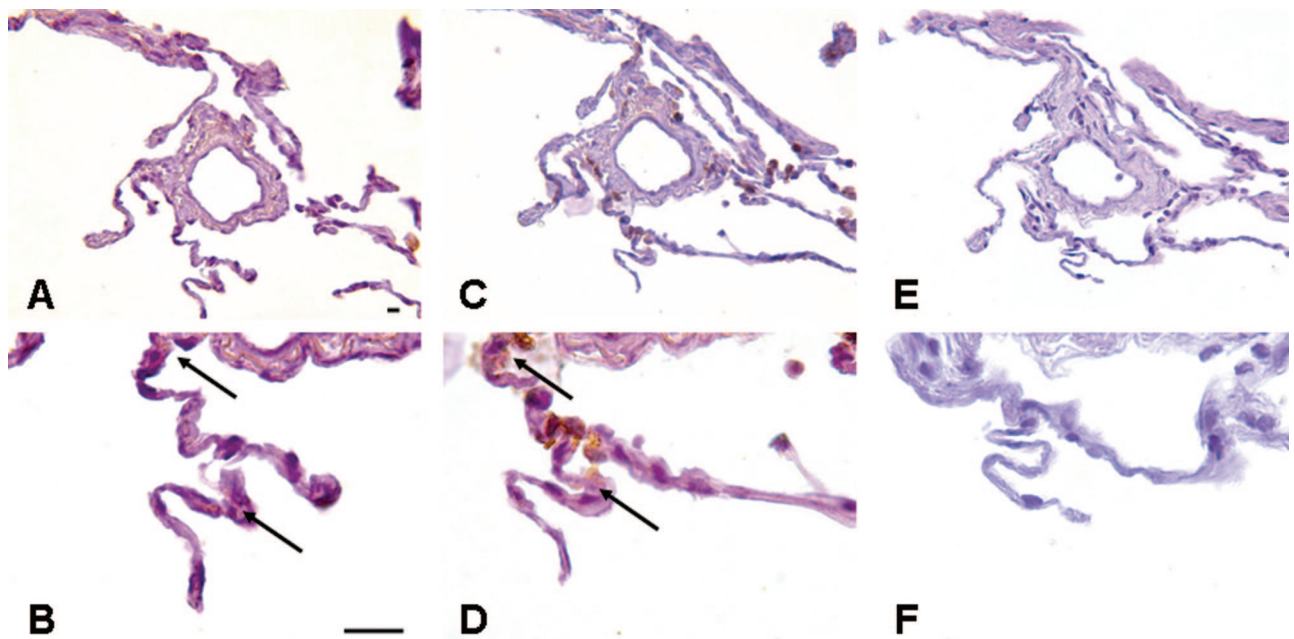


**Figure 6.** Normal lungs demonstrate Thy-1 staining in a pattern consistent with normal fibroblasts. **A–F:** Photomicrographs of serial sections from normal lung. **A, B:** IHC for Thy-1 (CD90). Dark brown staining is seen in cytoplasm and nuclei of spindle-shaped cells in the adventitia of a small blood vessel and in interstitium of alveolar septae (**arrows**). **C, D:** IHC for P4H. Dark brown staining is seen in a pattern similar to that observed for CD90. **E, F:** Control antiserum does not stain normal lung cells. Scale bar, 20  $\mu$ m. Original magnifications,  $\times 20$  (A, C, E);  $\times 100$  (B, D, F).

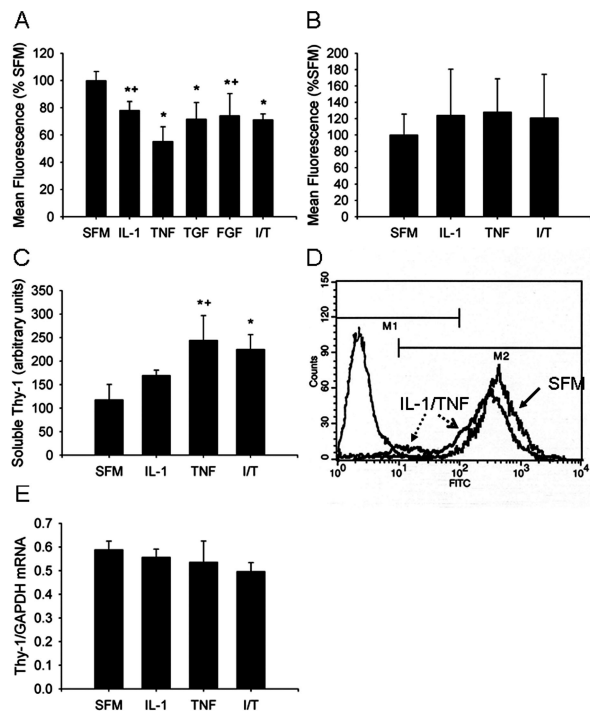


**Figure 7.** Fibrogenic cytokines induce loss of cell surface Thy-1 staining in lung fibroblasts and accumulation of soluble Thy-1 in conditioned medium. **A:** Normal lung fibroblasts were cultured in the presence of IL-1 $\beta$  (5 ng/ml), TNF- $\alpha$  (1 ng/ml), combined IL-1 $\beta$  and TNF- $\alpha$  (I/T, 5 ng/ml and 1 ng/ml, respectively), FGF-1 (20 ng/ml), or TGF- $\beta$  (1 ng/ml) for 96 hours, with fresh cytokine-containing medium or SFM replaced daily. Cells were resuspended, stained with anti-CD90 FITC, and analyzed by flow cytometry. The mean FITC fluorescence of the positive population (eg, M2 in **D**) was averaged for  $n = 3$  per condition and expressed relative to values for SFM-exposed cells, arbitrarily set at 100%. \* $P < 0.001$  versus SFM; + $P < 0.001$  versus TNF;  $\hat{P} < 0.001$  versus TNF and  $P = 0.007$  versus IL-1. **B:** After 96 hours of cytokine exposure, monolayers were washed three times with SFM and cultured for an additional 72 hours in SFM alone, then resuspended and analyzed by flow cytometry. The mean FITC fluorescence for the positive population was averaged and expressed relative to values for SFM-exposed cells, arbitrarily set at 100%. **C:** Thy-1 was immunoprecipitated from conditioned media of fibroblasts exposed to IL-1 $\beta$  (5 ng/ml), TNF- $\alpha$  (1 ng/ml), or combined IL-1 $\beta$  and TNF- $\alpha$  (T+I, 5 ng/ml and 1 ng/ml, respectively) for 72 hours, as above. Band density of enhanced chemiluminescent images was averaged for three separate experiments. Bars represent mean  $\pm$  SD. \* $P < 0.05$  versus SFM; + $P < 0.05$  versus IL-1. **D:** Normal fibroblasts were cultured in the presence of IL-1 and TNF (5 and 1 ng/ml, respectively) for 72 hours. CD90 expression was analyzed by flow cytometry. A representative histogram indicated by **solid arrow** indicates CD90 staining of SFM-exposed cells, the histogram indicated by **broken arrows** indicates IL-1/TNF-exposed cells, the histogram at the **far left** indicates SFM-exposed cells stained with isotype control Ab. **Dashed arrow, open arrowhead** indicates leftward shift of FITC staining intensity and **dotted arrow, closed arrowhead** indicates negatively staining cells. **E:** RNA was prepared from fibroblasts cultured in the presence of IL-1 and/or TNF for 6 hours and subjected to RT-PCR using primers specific for human Thy-1 and GAPDH as described in Materials and Methods. Histogram depicts the ratio of band intensity for Thy-1/GAPDH PCR products averaged for three experiments.

### Loss of Thy-1 Surface Expression in Human Lung Fibroblasts Is Associated with Increased $\alpha$ -SMA Expression and Increased Phosphorylation of Smad 2/3

To determine whether the observed *in vitro* loss of Thy-1 expression in fibroblasts was associated with similar biological changes to those observed *in vivo*, we performed immunofluorescent staining for Thy-1 and  $\alpha$ -SMA, and immunoblotting for  $\alpha$ -SMA, pSmad 2/3,

**Table 1.** Decrease in Thy-1 Expression Induced by IL-1 $\beta$  and TNF- $\alpha$  at 72 Hours

Fibroblast line	% Thy-1 versus SFM control (SD)	<i>P</i> value
Human foreskin	71.2 (4.3)	0.004
Human lung (LN-1)	70.4 (9.5)	0.038
Human lung (VF)	85.4 (6.8)	0.035
Human lung (HNL-1)	79.9 (3.4)	0.014

and total Smad, in normal lung fibroblasts after 72 hour exposure to IL-1 and TNF, individually and in combination. At baseline, the majority of normal fibroblasts expressed Thy-1 (green cell surface staining; Figure 8A). Faint  $\alpha$ -SMA staining was seen, predominantly in fibroblasts with low or absent Thy-1 expression (red intracellular staining). After 72-hour cytokine stimulation, Thy-1 expression is decreased or absent in many fibroblasts, concurrent with increased  $\alpha$ -SMA expression (Figure 8; B to D). Immunoblots confirmed increased  $\alpha$ -SMA expression (Figure 8E), and indicated increased TGF- $\beta$  signaling, as demonstrated by an increased ratio of phosphorylated to total Smad, concurrent with shedding of Thy-1 (Figure 8F).

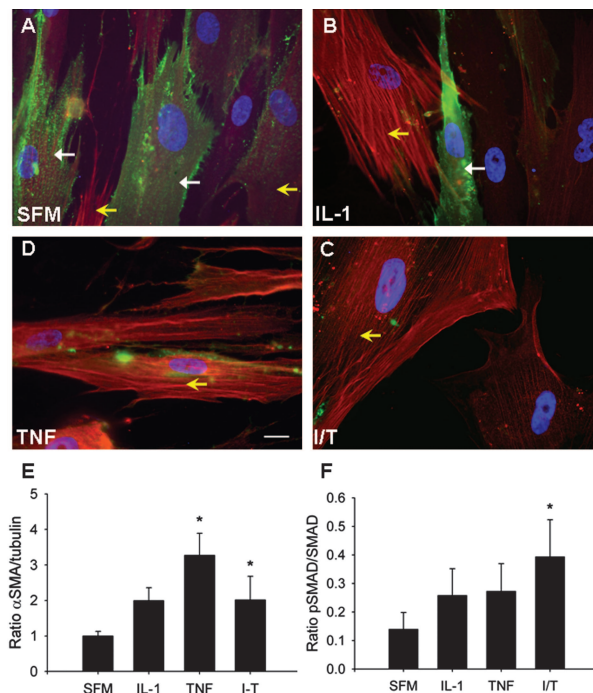


**Figure 8.** Loss of Thy-1 expression in human lung fibroblasts correlates with increased expression of  $\alpha$ -SMA and pSmad 2/3. Normal lung fibroblasts were cultured in the presence of IL-1 $\beta$  and TNF- $\alpha$ , alone or in combination, as in Figure 7, above, for 72 hours. **A–D:** Immunofluorescence photomicrographs of fibroblasts grown on coverslips and stained with FITC-conjugated Thy-1 antibody and Cy3-conjugated  $\alpha$ -SMA antibody. **Closed arrows** indicate cell-surface Thy-1 expression (green), **open yellow arrows** indicate intracellular  $\alpha$ -SMA (red). **E** and **F:** Densitometric analysis of immunoblots for  $\alpha$ -SMA (expressed as ratio to tubulin, **E**) and pSmad2/3 (expressed as a ratio to total Smad, **F**). \* $P < 0.05$  versus SFM. Scale bar, 20  $\mu$ m. Original magnifications,  $\times 63$ .

## Discussion

The clinical impact of fibrotic diseases and their resistance to treatment have generated an intense search for biological modifiers of fibrogenesis. Findings reported here suggest that the absence of Thy-1 in fibroblasts correlates with a more fibrotic phenotype *in vivo*, both in the BL model and in human IPF, as well as *in vitro*. These findings are consistent with our previous studies demonstrating higher proportions of Thy-1-negative lung fibroblasts in rat strains with higher susceptibility to BL-induced fibrosis, and increased fibroproliferation *in vitro* in Thy-1-negative lung fibroblasts in response to platelet-derived growth factor-AA, IL-1, and connective tissue growth factor.<sup>12,13,32</sup> Thy-1<sup>-/-</sup> mice have a higher accumulation of collagen and worse fibrosis 2 weeks after intratracheal BL, as well as evidence of extensive TGF- $\beta$  activation. WT mice demonstrate TGF- $\beta$  activation, proliferation, and myofibroblast differentiation in Thy-1-negative cells that predominate in fibrotic areas. In humans, within fibroblastic foci characteristic of UIP, myofibroblasts are negative for Thy-1, unlike the majority of normal lung fibroblasts. Inflammatory and fibrogenic cytokines and growth factors down-regulate Thy-1 expression in normal human lung and skin fibroblasts *in vitro*, with accumulation of soluble Thy-1 in conditioned media suggesting shedding of cell-surface Thy-1, concurrent with increased TGF- $\beta$  signaling and  $\alpha$ -SMA expression. These findings confirm a significant role for a Thy-1-negative subpopulation of lung fibroblasts in lung fibrosis, and strongly support the possibility that early injury/inflammatory events lead to the emergence and persistence of a profibrotic, Thy-1-negative myofibroblastic subpopulation.

Fibroblast Thy-1 subpopulations with differing phenotypes have been isolated from other tissues, such as spleen and orbital soft tissues.<sup>33,34</sup> The subsets, when sorted using magnetic beads or flow cytometry, remain stable through many passages in culture. However, the significance of Thy-1 expression with regard to fibrosis has not been determined. Thy-1 is a glycoposphatidylinositol (GPI)-linked cell-surface glycoprotein expressed on subsets of neurons, hematopoietic/immune cells, and fibroblasts. Thy-1 interacts in lipid rafts with multiple signaling intermediates important in regulating cell adhesion and cytoskeletal reorganization necessary for migration.<sup>35-38</sup> The consequences of fibroblast Thy-1 expression are less well known, but our previous studies indicate that Thy-1 modulates intracellular signaling critical to fibroproliferation,<sup>12,13,32</sup> cell adhesion, cell migration, and cytoskeletal reorganization.<sup>39,40</sup> Recent *in vitro* data show that activation of latent TGF- $\beta$  and increased myofibroblastic differentiation in response to inflammatory signals occur exclusively in Thy-1-negative rat lung fibroblasts,<sup>14</sup> consistent with findings reported here *in vivo* and *in vitro* in human lung fibroblasts.

Thy-1<sup>-/-</sup> mice have a normal life expectancy, alterations in hippocampal long-term potentiation and mildly impaired cutaneous immunity.<sup>19,41,42</sup> These findings are consistent with known roles of Thy-1 in neurite outgrowth, which could affect central nervous system development, and in modulating adhesion and signaling in lymphocytic

cells. Before the current study, fibroproliferative responses have not been studied in Thy-1<sup>-/-</sup> mice. Because in these mice Thy-1 is absent from all cells that would otherwise express it, it is possible that the differences we observe are not due solely to changes in fibroblast Thy-1 expression. Negative testing for a comprehensive panel of infectious agents in these mice, as well as the absence of lung pathology in saline-treated Thy-1<sup>-/-</sup> controls, indicate that the differences we observed are not likely to be the result of differential infection with respiratory pathogens arising from altered host defense. Because Thy-1 is expressed on murine lymphocytes, it is possible that differences in inflammation between Thy-1<sup>-/-</sup> mice and WT mice could affect fibrotic responses to BL. BL administration results in an inflammatory response, although the role of lymphocytic inflammation in the BL response is controversial, as is the role of inflammation in IPF.<sup>43,44</sup> BL-induced fibrosis is observed in lymphocyte-depleted mice.<sup>45</sup> In the studies reported here, histopathological scoring of inflammation was increased in both WT and Thy-1<sup>-/-</sup> mice at 14 days, with no significant differences in the two groups (data not shown). Given the well-characterized role of fibroblasts in fibroproliferation and collagen deposition, and the previously described profibrotic phenotype of Thy-1-negative fibroblasts *in vitro*, it is likely that absence of Thy-1 expression on fibroblasts is what predisposes Thy-1<sup>-/-</sup> mice to more severe fibrosis.

In IPF, a paradigmatic and pernicious form of lung fibrosis in humans, one of the most rigorous clinical correlates of a poor prognosis is the presence of fibroblastic foci at histopathology.<sup>2-5</sup> These are thought to represent collections of interstitial fibroblasts with persistent activation of wound healing functions, such as proliferation and matrix elaboration (granulation tissue or young connective tissue). The origin and nature of these fibroblasts is unknown, although certain features, such as  $\alpha$ -SMA expression, have been characterized and are consistent with fibroproliferative fibroblasts in other tissues, such as granulating wounds.<sup>46</sup> We hypothesized, based on studies in our laboratory and others, that these would be predominantly Thy-1-negative. Our findings indicate absent Thy-1 staining in spindle-shaped cells that are mostly P4H and PCNA-positive in fibroblastic foci. Thy-1 can be expressed in smooth muscle cells and is inducible in endothelial cells.<sup>47</sup> Thy-1 staining is seen in small blood vessels in human IPF sections in our study, confirming that absence of staining in fibroblastic foci is not artifactual. A well-established feature of fibrotic fibroblasts in lung and other tissues is expression of  $\alpha$ -SMA and enhanced contractility, indicating a myofibroblastic phenotype.<sup>48</sup> As expected, fibroblasts in foci in our study samples expressed  $\alpha$ -SMA. Furthermore,  $\alpha$ -SMA expression was seen in Thy-1-negative cells in fibrotic areas in the BL model, and loss of Thy-1 correlated with increased  $\alpha$ -SMA expression *in vitro*. These findings differ from those of a recent study in orbital and myometrial fibroblasts, which indicated that Thy-1-positive cells derived from the eye and uterus are more likely than Thy-1-negative cells to be myofibroblasts.<sup>49</sup>

Our findings reported here, including *in vivo* and *in vitro* data from both mice and humans, as well as recent *in vitro* studies in rat lung fibroblasts,<sup>14</sup> indicate that in lung fibroblasts Thy-1 and  $\alpha$ -SMA are discordant, suggesting that correlation of Thy-1 and  $\alpha$ -SMA is likely to be tissue-specific. Multiple published studies support heterogeneity of fibroblasts among different tissues.<sup>50</sup>

Our findings could be interpreted as demonstrating either that the presence of Thy-1 is protective or that its loss is pathogenic. Analysis of our data together with published studies favors the latter. First, we have shown that the majority of fibroblasts cultured from normal human lung are Thy-1-positive ( $91.7 \pm 8\%$ ). These proportions appear to represent the level of expression *in vivo*. Although there is no widely accepted fibroblast-specific marker, we have demonstrated Thy-1 staining in both normal lung and in uninvolved areas of lung in UIP, in a pattern nearly identical to that seen with P4H, and consistent with the anatomical location of fibroblasts (interstitial septal areas and connective tissue surrounding small airways and blood vessels). Secondly, in other model systems the loss of Thy-1 correlates with pathogenic alterations. Optic nerve injury results in down-regulated Thy-1 expression in retinal ganglion cells.<sup>51</sup> Oncogenic transformation of 3T3 cells with ras proto-oncogene results in internalization of Thy-1 associated with acquisition of an anchorage-independent phenotype.<sup>52</sup> Thy-1 can also be shed from the cell surface, and this mechanism has been demonstrated in fibroblastic synovocytes in inflamed joints in rheumatoid arthritis.<sup>53</sup> Thirdly, we have demonstrated a shift from Thy-1 positive to negative associated with pathogenic alterations *in vivo* (UIP, BL) and *in vitro* (cytokine exposure). Thy-1 expression decreases with exposure to IL-1 $\beta$ , TNF- $\alpha$ , and IL-1 and TNF in combination. We have also observed loss of Thy-1 in response to TGF- $\beta$  and fibroblast growth factor (FGF)-1. Decreases in response to IL-1 and TNF were first discernible at 24 hours (not shown) and continued up to 96 hours. Flow cytometry histograms showed both leftward shift in Thy-1 profile of Thy-1-positive cells and emergence of a Thy-1-negative subpopulation. Shedding of Thy-1 appeared to be a prominent mechanism for the loss of Thy-1 observed. Thy-1 was recovered from conditioned media of cultured fibroblasts by immunoprecipitation, and the amount increased with exposure to the above-named mediators, at both 6 and 12 hours, with TNF- $\alpha$  having the most pronounced effect. Accumulation in conditioned media correlated temporally with loss from the cell surface detected by flow cytometry. The degree of shedding and time course we observed is similar to that recently reported for Thy-1 shedding from fibroblasts induced by human cytomegalovirus infection.<sup>54</sup> Interestingly, human cytomegalovirus and other herpesvirus family members have been implicated in the pathogenesis of IPF.<sup>55</sup> Other potential mechanisms of Thy-1 loss, such as internalization/degradation or decreased transcription are less likely to underlie changes seen at 6 and 12 hours, but may come into play at later time points. We were unable to detect changes in mRNA at 6 and 12 hours.

The *in vitro* shedding of Thy-1 throughout 72 to 96 hours is associated with significant biological changes in lung fibroblasts, namely increased endogenous TGF- $\beta$  signaling as demonstrated by Smad phosphorylation, and increased expression of  $\alpha$ -SMA, suggesting myofibroblastic differentiation. In the relatively short time frame imposed by experimental conditions, the loss of Thy-1 is incomplete and transient. *In vivo*, in the setting of prolonged cytokine exposure, interaction with other cell types, and an altered matrix milieu, shedding of Thy-1 could initiate a more permanent shift toward a Thy-1-negative, profibrotic myofibroblast phenotype.

Our findings indicate that loss of fibroblast Thy-1 expression appears to be an important mechanism in lung fibrogenesis. An initiating event, unknown in the case of IPF, triggers release of fibrogenic mediators from parenchymal or immune/inflammatory cells, which then mediates loss of fibroblast cell surface Thy-1. Thy-1-negative fibroblasts, which are more sensitive to growth factors, such as platelet-derived growth factor-AA and connective tissue growth factor, may selectively proliferate and accumulate in early fibrogenic lesions, and may then persist through autocrine signaling. Furthermore, based on the differential cellular morphology of Thy-1 subpopulations, and the known effects of Thy-1 on adhesion and motility in lymphocytic and neuronal cells, Thy-1-negative fibroblasts may preferentially migrate into provisional matrix and form the nidus for development of fibroblastic foci. Thus the cell surface glycoprotein Thy-1 is likely to be an important regulator of fibrogenic responses in fibroblasts. Delineation of the molecular mechanisms involved and the role of Thy-1 fibroblast subpopulations in other fibrotic conditions should yield novel insights into the molecular pathogenesis of fibrosis.

### Acknowledgments

We thank the UAB Hospital Anatomical Pathology Laboratories and the Comparative Medicine Histopathology Service for preparation and sectioning of paraffin blocks and performing immunohistochemical, H&E, picrosirius red, and Masson's trichrome staining; the UAB Flow Cytometry Core for providing assistance with cytometry and analysis; the UAB Center for Metabolic Bone Disease Laboratory (Patty Lott and Dezhi Wang) for providing assistance with morphometric analysis of picrosirius red-stained specimens; Drs. Joanne Murphy-Ullrich and Yong Zhou for helpful discussions concerning TGF- $\beta$ -associated methodologies and interpretation of results; Drs. Kaiyu Yuan, Namasivayam Ambalavanan, and Lance Prince for technical assistance; Dr. Joseph A. Lasky for helpful discussions regarding experimental design and data interpretation; Lindsay M. Swain and Cassie Woodley for assistance with manuscript preparation; and Dr. Gerald M. Fuller for his critical reading of the manuscript.

## References

1. Crystal RG, Bitterman PB, Mossman B, Schwarz MI, Sheppard D, Almsy L, Chapman HA, Friedman SL, King Jr TE, Leinwand LA, Liotta L, Martin GR, Schwartz DA, Schultz GS, Wagner CR, Musson RA: Future research directions in idiopathic pulmonary fibrosis: summary of a National Heart, Lung, and Blood Institute working group. *Am J Respir Crit Care Med* 2002, 166:236–246
2. King TE, Schwarz MI, Brown K, Tooze JA, Colby TV, Waldron JA, Flint A, Thurlbeck W, Cherniack RM: Idiopathic pulmonary fibrosis. Relationship between histopathologic features and mortality. *Am J Respir Crit Care Med* 2001, 164:1025–1032
3. Nicholson AG, Fulford LG, Colby TV, du Bois RM, Hansell DM, Wells AU: The relationship between individual histologic features and disease progression in idiopathic pulmonary fibrosis. *Am J Respir Crit Care Med* 2002, 166:173–177
4. Katzenstein AL, Myers JL: Idiopathic pulmonary fibrosis: clinical relevance of pathologic classification. *Am J Respir Crit Care Med* 1998, 157:1301–1315
5. Selman M, King TE, Pardo A: Idiopathic pulmonary fibrosis: prevailing and evolving hypotheses about its pathogenesis and implications for therapy. *Ann Intern Med* 2001, 134:136–151
6. Worrall JG, Whiteside TL, Prince RK, Buckingham RB, Stachura I, Rodnan GP: Persistence of scleroderma-like phenotype in normal fibroblasts after prolonged exposure to soluble mediators from mononuclear cells. *Arthritis Rheum* 1986, 29:54–64
7. Raghu G, Chen Y, Rusch V, Rabinovitch PS: Differential proliferation of fibroblasts cultured from normal and fibrotic human lungs. *Am Rev Respir Dis* 1988, 138:703–708
8. Torry DJ, Richards CD, Podor TJ, Gaudie J: Anchorage-independent colony growth of pulmonary fibroblasts derived from fibrotic human lung tissue. *J Clin Invest* 1994, 93:1525–1532
9. Phipps RP (Ed): *Pulmonary Fibroblast Heterogeneity*. Boca Raton, CRC Press, 1992
10. Phipps RP, Penney DP, Keng P, Quill H, Paxhia A, Derdak S, Felch ME: Characterization of two major populations of lung fibroblasts: distinguishing morphology and discordant display of Thy 1 and class II MHC. *Am J Respir Cell Mol Biol* 1989, 1:65–74
11. Phipps RP, Baecher C, Frelinger JG, Penney DP, Keng P, Brown D: Differential expression of interleukin 1 $\alpha$  by Thy-1<sup>+</sup> and Thy-1<sup>-</sup> lung fibroblast subpopulations: enhancement of interleukin 1 $\alpha$  production by tumor necrosis factor- $\alpha$ . *Eur J Immunol* 1990, 20:1723–1727
12. Hagood JS, Miller PJ, Lasky JA, Tousson A, Guo B, Fuller GM, McIntosh JC: Differential expression of platelet-derived growth factor- $\alpha$  receptor by Thy-1(-) and Thy-1(+) lung fibroblasts. *Am J Physiol* 1999, 277:L218–L224
13. Hagood JS, Lasky JA, Nesbitt JE, Segarini P: Differential expression, surface binding, and response to connective tissue growth factor in lung fibroblast subpopulations. *Chest* 2001, 120:S64–S66
14. Zhou Y, Hagood JS, Murphy-Ullrich JE: Thy-1 expression regulates the ability of rat lung fibroblasts to activate transforming growth factor- $\beta$  in response to fibrogenic stimuli. *Am J Pathol* 2004, 165:659–669
15. Schuyler M, Cormier Y: The diagnosis of hypersensitivity pneumonitis. *Chest* 1997, 111:534–536
16. Bronchoalveolar lavage constituents in healthy individuals, idiopathic pulmonary fibrosis, and selected comparison groups. The BAL Cooperative Group Steering Committee. *Am Rev Respir Dis* 1990, 141:S169–S202
17. Coleman A, Colby TV: Histologic diagnosis of extrinsic allergic alveolitis. *Am J Surg Pathol* 1988, 12:514–518
18. Flanders KC, Thompson NL, Cissel DS, Van Obberghen-Schilling E, Baker CC, Kass ME, Ellingsworth LR, Roberts AB, Sporn MB: Transforming growth factor- $\beta$  1: histochemical localization with antibodies to different epitopes. *J Cell Biol* 1989, 108:653–660
19. Nosten-Bertrand M, Errington ML, Murphy KP, Tokugawa Y, Barboni E, Kozlova E, Michalovich D, Morris LR, Silver J, Stewart CL, Bliss TV, Morris RJ: Normal spatial learning despite regional inhibition of LTP in mice lacking Thy-1. *Nature* 1996, 379:826–829
20. Wang R, Ibarra-Sunga O, Verliński L, Pick R, Uhal BD: Abrogation of bleomycin-induced epithelial apoptosis and lung fibrosis by captopril or by a caspase inhibitor. *Am J Physiol* 2000, 279:L143–L151
21. Brey EM, Lalani Z, Johnston C, Wong M, McIntire LV, Duke PJ, Patrick Jr CW: Automated selection of DAB-labeled tissue for immunohistochemical quantification. *J Histochem Cytochem* 2003, 51:575–584
22. Chantrain CF, DeClerck YA, Groshen S, McNamara G: Computerized quantification of tissue vascularization using high-resolution slide scanning of whole tumor sections. *J Histochem Cytochem* 2003, 51:151–158
23. Berg RA: Determination of 3- and 4-hydroxyproline. *Methods Enzymol* 1982, 82:372–398
24. Davis JK, Thorp RB, Parker RF, White H, Dziedzic D, D'Arcy J, Cassell GH: Development of an aerosol model of murine respiratory mycoplasmosis in mice. *Infect Immun* 1986, 54:194–201
25. Pinson DM, Schoeb TR, Lindsey JR, Davis JK: Evaluation by scoring and computerized morphometry of lesions of early *Mycoplasma pulmonis* infection and ammonia exposure in F344/N rats. *Vet Pathol* 1986, 23:550–555
26. Roberts AB, Russo A, Felici A, Flanders KC: Smad3: a key player in pathogenetic mechanisms dependent on TGF- $\beta$ . *Ann NY Acad Sci* 2003, 995:1–10
27. Selman M: Plunging into the chaos of the cytokine/chemokine cocktail in pulmonary fibrosis: how many and how important are they? *Am J Respir Crit Care Med* 2003, 168:730–731
28. Lechleider RJ, de Caestecker MP, Dehejia A, Polymeropoulos MH, Roberts AB: Serine phosphorylation, chromosomal localization, and transforming growth factor- $\beta$  signal transduction by human bsp-1. *J Biol Chem* 1996, 271:17617–17620
29. Kontinen YT, Nykanen P, Nordstrom D, Saari H, Sandelin J, Santavirta S, Kouri T: DNA synthesis in prolyl 4-hydroxylase positive fibroblasts in situ in synovial tissue. An autoradiography-immunoperoxidase double labeling study. *J Rheumatol* 1989, 16:339–345
30. Esterre P, Melin M, Serran M, Grimaud J-A: New specific markers of human and mouse fibroblasts. *Cell Mol Biol* 1992, 38:297–301
31. Renzoni EA, Walsh DA, Salmon M, Wells AU, Sestini P, Nicholson AG, Veeraraghavan S, Bishop AE, Romanska HM, Pantelidis P, Black CM, Du Bois RM: Interstitial vascularity in fibrosing alveolitis. *Am J Respir Crit Care Med* 2003, 167:438–443
32. Hagood JS, Mangalwadi A, Guo B, MacEwen MW, Salazar L, Fuller GM: Concordant and discordant interleukin-1-mediated signaling in lung fibroblast thy-1 subpopulations. *Am J Respir Cell Mol Biol* 2002, 26:702–708
33. Borrello MA, Phipps RP: Differential Thy-1 expression by splenic fibroblasts defines functionally distinct subsets. *Cell Immunol* 1996, 173:198–206
34. Smith TJ, Sempowski GD, Wang H-S, DelVecchio PJ, Lippe SD, Phipps RP: Evidence for cellular heterogeneity in primary cultures of human orbital fibroblasts. *J Clin Endocrinol Metab* 1995, 80:2620–2625
35. Simons K, Toomre D: Lipid rafts and signal transduction. *Nat Rev Mol Cell Biol* 2000, 1:31–39
36. Krauss K, Altevogt P: Integrin leukocyte function-associated antigen-1-mediated cell binding can be activated by clustering of membrane rafts. *J Biol Chem* 1999, 274:36921–36927
37. Laux T, Fukami K, Thelen M, Golub T, Frey D, Caroni P: GAP43, MARCKS, and CAP23 modulate PI(4,5)P<sub>2</sub> at plasmalemmal rafts, and regulate cell cortex actin dynamics through a common mechanism. *J Cell Biol* 2000, 149:1455–1472
38. Aarts LH, Verkade P, van Dalen JJ, van Rozen AJ, Gispen WH, Schrama LH, Schotman P: B-50/GAP-43 potentiates cytoskeletal reorganization in raft domains. *Mol Cell Neurosci* 1999, 14:85–97
39. Barker TH, Grenett HE, MacEwen MW, Tilden SG, Fuller GM, Settleman J, Woods A, Murphy-Ullrich J, Hagood JS: Thy-1 regulates fibroblast focal adhesions, cytoskeletal organization and migration through modulation of p190 RhoGAP and Rho GTPase activity. *Exp Cell Res* 2004, 295:488–496
40. Barker TH, Pallero MA, MacEwen MW, Tilden SG, Woods A, Murphy-Ullrich JE, Hagood JS: Thrombospondin-1-induced focal adhesion disassembly in fibroblasts requires Thy-1 surface expression, lipid raft integrity, and Src activation. *J Biol Chem* 2004, 279:23510–23516
41. Mayeux-Portas V, File SE, Stewart CL, Morris RJ: Mice lacking the cell adhesion molecule Thy-1 fail to use socially transmitted cues to direct their choice of food. *Curr Biol* 2000, 10:68–75
42. Beissert S, He HT, Hueber AO, Lellouch AC, Metzke D, Mehling A, Luger TA, Schwarz T, Grabbe S: Impaired cutaneous immune responses in Thy-1-deficient mice. *J Immunol* 1998, 161:5296–5302
43. Kradin RL, Sakamoto H, Jain F, Zhao LH, Hymowitz G, Preffer F: IL-10

- inhibits inflammation but does not affect fibrosis in the pulmonary response to bleomycin. *Exp Mol Pathol* 2004, 76:205–211
44. Gauldie J: Proinflammatory mechanisms are a minor component of the pathogenesis of idiopathic pulmonary fibrosis. *Am J Respir Crit Care Med* 2002, 165:1205–1206
  45. Janick-Buckner D, Ranges GE, Hacker MP: Effect of cytotoxic monoclonal antibody depletion of T-lymphocyte subpopulations on bleomycin-induced lung damage in C57BL/6J mice. *Toxicol Appl Pharmacol* 1989, 100:474–484
  46. Shahar I, Fireman E, Topilsky M, Grief J, Schwarz Y, Kivity S, Ben-Efraim S, Spirer Z: Effect of endothelin-1 on alpha-smooth muscle actin expression and on alveolar fibroblasts proliferation in interstitial lung diseases. *Int J Immunopharmacol* 1999, 21:759–775
  47. Lee WS, Jain MK, Arkonac BM, Zhang D, Shaw SY, Kashiki S, Maemura K, Lee SL, Hollenberg NK, Lee ME, Haber E: Thy-1, a novel marker for angiogenesis upregulated by inflammatory cytokines. *Circ Res* 1998, 82:845–851
  48. Phan SH: Fibroblast phenotypes in pulmonary fibrosis. *Am J Respir Cell Mol Biol* 2003, 29:S87–S92
  49. Koumas L, Smith TJ, Feldon S, Blumberg N, Phipps RP: Thy-1 expression in human fibroblast subsets defines myofibroblastic or lipofibroblastic phenotypes. *Am J Pathol* 2003, 163:1291–1300
  50. Chang HY, Chi JT, Dudoit S, Bondre C, van de Rijn M, Botstein D, Brown PO: Diversity, topographic differentiation, and positional memory in human fibroblasts. *Proc Natl Acad Sci USA* 2002, 99:12877–12882
  51. Schlamp CL, Johnson EC, Li Y, Morrison JC, Nickells RW: Changes in Thy1 gene expression associated with damaged retinal ganglion cells. *Mol Vis* 2001, 7:192–201
  52. Sugimoto Y, Ikawa Y, Nakauchi H: Thy-1 as a negative growth regulator in ras-transformed mouse fibroblasts. *Cancer Res* 1991, 51:99–104
  53. Saalbach A, Wetzig T, Hausteil UF, Anderegg U: Detection of human soluble Thy-1 in serum by ELISA. Fibroblasts and activated endothelial cells are a possible source of soluble Thy-1 in serum. *Cell Tissue Res* 1999, 298:307–315
  54. Leis M, Marschall M, Stamminger T: Downregulation of the cellular adhesion molecule Thy-1 (CD90) by cytomegalovirus infection of human fibroblasts. *J Gen Virol* 2004, 85:1995–2000
  55. Tang YW, Johnson JE, Browning PJ, Cruz-Gervis RA, Davis A, Graham BS, Brigham KL, Oates Jr JA, Loyd JE, Stecenko AA: Herpesvirus DNA is consistently detected in lungs of patients with idiopathic pulmonary fibrosis. *J Clin Microbiol* 2003, 41:2633–2640